Rhodocomatulin-Type Anthraquinones from the Australian Marine Invertebrates Clathria hirsuta and Comatula rotalaria

Rhodocomatulin-type Anthraquinones from the Australian Marine Invertebrates *Clathria hirsuta* and *Comatula rotalaria*

Shahan Khokhar,[†] Gregory K. Pierens,[‡] John N. A. Hooper,[†,§] Merrick G. Ekins,[§] Yunjiang Feng,[†,*] and Rohan A. Davis[†,*]

[†]*Eskitis Institute, Griffith University, Brisbane, QLD 4111, Australia.*

[‡]*Centre for Advanced Imaging, The University of Queensland, Brisbane, QLD 4072, Australia*

[§]*Queensland Museum, South Brisbane, QLD 4101, Australia.*

ABSTRACT

Chemical investigations of an Australian sponge, *Clathria hirsuta*, from the Great Barrier Reef, have resulted in the isolation of two known anthraquinones, rhodocomatulin 5,7-dimethyl ether (**1**) and rhodocomatulin 7-methyl ether (**2**). Additionally, four new anthraquinone metabolites, 6-methoxy-rhodocomatulin 7-methyl ether, 3-bromo-6-methoxy-12-desethyl-rhodocomatulin 7-methyl ether, 3-bromo-6-methoxy-rhodocomatulin 7-methyl ether and 3-bromo-rhodocomatulin 7-methyl ether (**3**–**6**) were also isolated and characterized. This is the first report of the rhodocomatulin-type anthraquinones from a marine sponge, as **1** and **2** were previously isolated from the marine crinoid genus *Comatula*. An additional chemical investigation of the marine crinoid *Comatula rotalaria* enabled the isolation of further quantities of **1** and **2**, as well as two additional new crinoid metabolites, 12-desethyl-rhodocomatulin 5,7-dimethyl ether and 12-desethyl-rhodocomatulin 7-methyl ether (**7** and **8**). An NMR spectroscopic analysis of compounds **7** and **8** provided further insight into the rhodocomatulin planar structure, and together with the successful implementation of DFT-NMR calculations, confirmed that the rhodocomatulin metabolites existed as *para* rather than *ortho* quinones.

Marine sponges continue to yield structurally complex, unusual and bioactive natural products.[1] The genus *Clathria* has been the source of a number of compounds spanning several secondary metabolite classes, including terpenoids (e.g., phorone B and gombaspiroketals),[2,3] alkaloids (e.g., mirabilins and araisoamines),[4-6] peptides (e.g., the microcionamides)[7] and chemicals of mixed biosynthetic origin (e.g., the clathrins).[8] The chemical diversity sourced from this sponge genus can now be extended to include polyketide-derived anthraquinones. The anthraquinones obtained during our chemical investigations of the extract of the Australian sponge, *Clathria hirsuta*, comprised the known compounds rhodocomatulin 5,7-dimethyl ether (**1**) and rhodocomatulin 7-methyl ether (**2**), which were first isolated from the marine crinoid genus *Comatula* (Phylum Echinodermata) during the 1960s.[9,10] The structures of these two compounds were originally determined through UV-Vis spectrophotometry, MS analysis, chemical degradation experiments, comparison of TLC-retention times to known quinone standards and early ^{1}H NMR experiments.[9,10] A total synthesis of these metabolites was also reported in the 1980s, however only ^{1}H NMR data was provided to support the structures.[9,10] In this paper, we provide the full NMR spectroscopic characterization (^{13}C and 2D NMR) of compounds **1** and **2**, as well as the structure elucidation of four new, minor anthraquinone metabolites from *Clathria hirsuta*, 6-methoxy-rhodocomatulin 7-methyl ether, 3-bromo-6-methoxy-12-desethyl-rhodocomatulin 7-methyl ether, 3-bromo-6-methoxy-rhodocomatulin 7-methyl ether and 3-bromo-rhodocomatulin 7-methyl ether (**3**–**6**). Determining the structures of these four new metabolites was particularly challenging, owing to the low ^{1}H:^{13}C ratio, paucity of material, number of non-protonated sp^{2} hybridized aromatic carbon atoms and the presence of a bromine atom in compounds **4**–**6**. Our interest in the rhodocomatulin class of anthraquinones led us to examine a specimen of the crinoid *Comatula rotalaria* for related compounds. This study afforded further quantities of **1**, suitable for biological testing, and

also yielded two additional new metabolites, 12-desethyl-rhodocomatulin 5,7-dimethyl ether and 12-desethyl-rhodocomatulin 7-methyl ether (**7** and **8**). The acquisition of **7** and **8** was fortuitous, as their spectroscopic analysis yielded further insights which allowed for the structural confirmation of the rhodocomatulin anthraquinone core.

RESULTS AND DISCUSSION

The specimen of *C. hirsuta* was freeze-dried, ground into a fine powder and exhaustively extracted with CH_2Cl_2 and then MeOH. The CH_2Cl_2 extract was found to contain a large amount of lipids by ^{1}H NMR analysis, and was thus discarded. The MeOH extract was then subjected to normal-phase (NP) DIOL-bonded silica gel flash column chromatography (stepwise gradient, *n*-hexane/EtOAc to MeOH). The fractions from this crude purification step were further purified by either NP-HPLC (*i*-PrOH/*n*-hexane) or RP-HPLC (MeOH/H_2O/0.1% TFA), which led to the isolation of compounds **1**–**6**.

Rhodocomatulin 5,7-dimethyl ether (**1**) was obtained as an orange gum. A full report of the structure elucidation by NMR spectroscopy is presented here because no ^{13}C and 2D NMR data has been recorded to date.[9,10] (–)-HRESIMS analysis of **1** indicated an ion consistent with a molecular formula of $C_{20}H_{18}O_7$. Ten distinct signals were noted in the ^{1}H NMR spectrum (Table 1): a shielded methyl triplet (δ_H 0.98), a methylene quartet of triplets (δ_H 1.67), an additional broad methylene triplet (δ_H 2.64), an aromatic methine singlet (δ_H 6.66), two methoxy singlets (δ_H 3.97 and 3.96), two *meta*-coupled methine doublets (δ_H 7.04 and 7.22, J = 2.5 Hz), and two exchangeable proton singlets (δ_H 13.61 and 11.33).

The ^{13}C NMR spectrum (Table 2) contained 20 signals, including five sp^3 carbons, 12 aromatic sp^2 carbons, and three carbonyl signals at δ_C 182.5 (C-9), 185.2 (C-10) and 203.4 (C-11). Analysis of the COSY spectrum (Figure 1) confirmed the *meta*-aromatic coupling, and also highlighted an additional spin system [δ_H 2.64 (H-12), 1.67 (H-13) and 0.98 (H-14)] corresponding to a propyl moiety. An HSQC spectrum enabled protons to be attached to their

respective carbons. The HMBC data (Figure 1) included a correlation from H-13 (δ_H 1.67) to C-11 (δ_C 203.4) that indicated the presence of a 1-oxobutyl moiety.

The existence of two highly substituted molecular fragments (fragment A and B, Figure 1) were established through analysis of the HMBC and ROESY correlations. Importantly, a series of connecting ROESY correlations from δ_H 7.22 (H-8) to δ_H 3.97 (7-OMe), from 7-OMe to δ_H 7.04 (H-6), and from H-6 to δ_H 3.96 (5-OMe), established the substitution pattern depicted (fragment A, Figure 1). HMBC correlations from the proton signal resonating at δ_H 7.22 (H-8) to the carbon at δ_C 182.5 (C-9), confirmed the presence of a benzenone-type system. ROESY correlations were also used to elucidate the substitution pattern of an additional system (fragment B, Figure 1). These included ROESY correlations from the phenolic proton at δ_H 13.61 (4-OH, deshielded because of hydrogen-bonding to the oxygen atom of C-10) to the aromatic methine proton at δ_H 6.66 (H-3), and from H-3 to an additional phenolic proton at δ_H 11.33 (2-OH). A weak HMBC correlation was also observed from δ_H 6.66 (H-3) to δ_C 185.2 (C-10), establishing the presence of a second benzenone type moiety (fragment B). Together with the 1-oxobutyl (fragment C, Figure 1), we were required to assemble three fragments into one structure. Two possible structures were consistent with the available NMR evidence: the *ortho* and *para* anthraquinone forms (Figure 1). At this point, we felt that the most likely candidate was the structure depicted as **1** (i.e., the *para* quinone), based on biosynthetic considerations (see Supporting Information). Spectroscopic and computational (DFT) investigations of additional metabolites reported later in this paper (**7** and **8**) provided further evidence of the *para* quinone. Compound **1** is a known metabolite, rhodocomatulin 5,7-dimethyl ether (from the marine crinoid genus *Comatula*) but to date, has had no ^{13}C and 2D NMR spectroscopic data reported.

Rhodocomatulin 7-methyl ether (**2**) was isolated as a pink powder. (–)-HRESIMS analysis of the sample gave an ion consistent with a molecular formula of $C_{19}H_{16}O_7$. Analysis

of the ^{1}H NMR spectrum (Table 1) revealed similarities between **1** and **2**. Important differences, however, included the loss of a methoxy singlet and the presence of an additional phenolic proton resonance at δ_H 12.15, which together with the molecular formula, suggested the absence of an *O*-methyl group at C-5 or C-7. ROESY correlations from H-8 (δ_H 7.12) to 7-OMe (δ_H 3.92), from 7-OMe to H-6 (δ_H 6.86), and from H-6 to the new phenolic singlet (5-OH, δ_H 12.15), indicated that position C-5 was hydroxylated in **2**. Thus, the chemical structure of compound **2** was assigned as rhodocomatulin 7-methyl ether, previously obtained from the crinoid *Comatula pectinata*.[10] This earlier study only provided UV, IR and ^{1}H NMR data, and was further confirmed through simple chemical degradation experiments.

The new metabolite **3** was isolated as an orange gum. (–)-HRESIMS analysis of **3** yielded an ion consistent with the molecular formula $C_{20}H_{18}O_8$, which corresponded to one extra oxygen atom compared with **1**. The ^{1}H NMR spectrum of **3** (Table 1) was similar to that of **1**, except for the presence of an additional exchangeable phenolic proton signal at δ_H 12.10, and only two non-coupling aromatic proton signals at δ_H 6.69 (H-3) and 7.33 (H-8). A ROESY experiment revealed δ_H 7.33 to be adjacent to 7-OMe (δ_H 3.99). This methoxy singlet coupled to C-7 (δ_C 158.0) in the HMBC spectrum. Interestingly, an HMBC correlation was observed from the other methoxy singlet (δ_H 3.85) to δ_C 141.2 (C-6), significantly shielded compared to the chemical shift of C-7 (δ_C 158.0). This chemical shift was consistent with a methoxylated aromatic carbon with two *ortho* oxygenated groups (i.e., 7-OMe and 5-OH).[11-13] HMBC correlations were observed from δ_H 7.33 (H-8) and 12.10 (5-OH) to δ_C 141.2 (C-6), thus confirming C-6 as a site of a methyl ether. HMBC correlations were also observed from H-8 and 5-OH to C-10a, confirming the substitution pattern depicted in **3** (Figure 3). Owing to the low quantity of material (0.1 mg), several carbon chemical shifts were not observed (i.e., C-2, C-8a, C-9a, C-10, C-11). Unfortunately, the low yields of the remaining molecules to be characterized (**4**–**6**) led to similar situations where not all ^{13}C

NMR shifts could be assigned (Table 2). Hence, the structure of 6-methoxy-rhodocomatulin 7-methyl ether was assigned as **3**.

The related new metabolite **4** was obtained as a brown/red gum. The (–)-LRESIMS spectrum showed an isotopic cluster of $[M - H]^-$ ions in the ratio of 1:1 at *m*/*z* 435 and 437, indicating the presence of one bromine atom. (–)-HRESIMS analysis yielded an ion consistent with the molecular formula $C_{18}H_{13}BrO_8$. The ^{1}H NMR spectrum of **4** was very similar to that of **3**, however now there was only one aromatic singlet (δ_H 7.37) and the propyl group was replaced by a methyl singlet (δ_H 2.42). The lack of an aromatic singlet in **4** compared to **3**, together with the molecular formula, indicated that one aromatic position was now brominated. No COSY correlations were observed, signifying that all protons were isolated from one another and not part of a spin-system. A ROESY experiment showed a correlation between δ_H 7.37 (H-8) and a methoxy group (δ_H 3.99, 7-OMe), suggesting that they were *ortho* to each other. The protons of the methoxy group (δ_H 3.85, 6-OMe) gave an HMBC correlation with a carbon atom resonating at δ_C 141.5 (C-6), suggesting that **4**, like **3**, was oxygenated at positions C-5, C-6 and C-7. ^{1}H NMR signals corresponding to the propyl chain seen in compounds **1**–**3** were no longer present. Instead, a methyl singlet at δ_H 2.42 (H-12) yielded an HMBC correlation with a ketone carbonyl at δ_C 200.4 (C-11), suggesting that C-1 was connected to a methyl ketone unit. C-3 was the only carbon atom remaining to which a heteroatom could be assigned. Thus, the structure of **4**, 3-bromo-6-methoxy-12-desethyl-rhodocomatulin 7-methyl ether, was established.

Compound **5** was isolated as an orange gum. Similar to **4**, the (–)-LRESIMS spectrum showed an isotopic cluster of $[M - H]^-$ ions in the ratio of 1:1 at *m*/*z* 463 and 465, indicating the presence of one bromine atom. (–)-HRESIMS gave an ion consistent with the molecular formula $C_{20}H_{17}BrO_8$. The ^{1}H NMR spectrum of **5** was almost identical to that of **3**, except the absence of an aromatic singlet was noted. In a similar manner to **4**, these data suggested that a

bromine atom was present on one of the aromatic rings. Further HMBC correlations from δ_H 7.34 (H-8) to δ_C 158.2 (C-7), 141.4 (C-6), 111.2 (C-10a), 181.0 (C-9) and 128.4 (C-8a) were consistent with the substitution pattern noted in **3**, with the bromine atom situated at position C-3. These data led to the structure, 3-bromo-6-methoxy-rhodocomatulin 7-methyl ether, being assigned to compound **5**.

The final molecule isolated from *Clathria hirsuta*, **6**, was acquired as a red gum. Again, the (–)-LRESIMS spectrum showed an isotopic cluster of $[M - H]^-$ ions in the ratio of 1:1 at *m*/*z* 433 and 435. The (–)-HRESIMS experiment gave an ion consistent with a molecular formula of $C_{19}H_{15}BrO_7$. The ^{1}H NMR spectrum of compound **6** was almost identical to that of **2**, except for the absence of an aromatic methine proton and one exchangeable proton. Similar arguments presented in the elucidation of **4** and **5** supported the idea that the bromine atom was also substituted at C-3 (δ_C 105.9). ROESY experiments provided evidence of the substitution pattern of C-6, C-7 and C-8; specifically, ROESY correlations were observed from H-8 (δ_H 7.16) to 7-OMe (δ_H 3.93), and 7-OMe to H-6 (δ_H 6.91). Although not observed in the ^{1}H NMR, an additional phenolic (OH) group was proposed at C-5; this accounted for the remaining oxygen and hydrogen atoms that had not been assigned, leading to the structure **6**, which we assigned the trivial name of 3-bromo-rhodocomatulin 7-methyl ether.

Due to our continuing interest in examining isolated natural products for cytotoxicity, we set out to acquire further amounts of the major component, **1**, for biological evaluation.[14,15] This led us to explore the featherstar genus *Comatula* as a source of the rhodocomatulin-type anthraquinones. An LC-MS analysis of the EtOH/H_2O (70:30) extract of a specimen of the featherstar *Comatula rotalaria*, collected in the Torres Strait, yielded molecular ions consistent with the molecular weights of both **1** and **2**. The extract was thus dried, and purified in the same manner as the *Clathria* extract (i.e., by DIOL-bonded silica

gel flash column chromatography and then NP-HPLC). This ultimately yielded sufficient quantities of **1**, enabling its testing against a panel of cancer cell lines: H460 (lung-cell carcinoma), SF-268 (human glioblastoma) and MCF-7 (breast-cell carcinoma). However, only limited (9%) growth inhibition towards MCF-7 (breast cell carcinoma) was observed at 10 μM after 72 h. Further amounts of **2** were also obtained, allowing the acquisition of a ^{13}C NMR spectrum (Table 2). In addition to **1** and **2**, two new and minor additional anthraquinones (**7** and **8**) from *C. rotalaria* were isolated.

Compound **7**, purified as an orange gum, yielded an ion consistent with a molecular formula of $C_{18}H_{14}O_7$ (*m*/*z* 341.0668 $[M - H]^-$) in the (–)-HRESIMS. The ^1H NMR spectrum of **7** (Table 3) was very similar to that of rhodocomatulin 5,7-dimethyl ether (**1**), however, the signals corresponding to the butyl chain in **1** were now absent. Instead, a singlet at δ_H 2.39 was present, consistent with a methyl ketone, previously observed in compound **4**. Analysis of the HMBC spectrum of **7** provided important information about the position of the alkyl side-chain relative to the anthraquinone core, correlations which had so far not been observed in compounds **1**–**6**. Specifically, HMBC correlations from δ_H 2.39 (H-12) to δ_C 124.9 (C-1) and from δ_H 6.67 (H-3) to C-1 confirmed that the methyl ketone was bonded through C-1. These considerations led to the structure of **7**, 12-desethyl-rhodocomatulin 5,7-dimethyl ether, being assigned.

Compound **8**, also obtained as an orange gum, showed an ion (*m*/*z* 327.0512, $[M - H]^-$) in the (–)-HRESIMS that corresponded to a molecular formula of $C_{17}H_{12}O_7$. The ^1H NMR spectrum was comparable to that of **2** (Table 3), however the butyl-chain proton signals were, again, absent. However, a methyl singlet at δ_H 2.40 was present, consistent with the methyl ketone group observed in **4** and **7**. Again, important HMBC correlations from δ_H 2.40 (H-12) to δ_C 126.6 (C-1) and from δ_H 6.70 (H-3) to C-1 confirmed that the methyl ketone was

bonded through C-1 (Figure 2). Ultimately, the NMR and MS data confirmed the structure of **8**, 12-desethyl-rhodocomatulin 7-methyl ether.

The isolation of **7** enabled the rhodocomatulin anthraquinone core to be easily confirmed by DFT-NMR methods. Specifically, we were able to verify that the rhodocomatulin class existed as *para* rather than *ortho* quinones (Figure 3). The truncated alkyl-chain of **7** compared to **1** greatly simplified the calculations and reduced computational times.[16] Our group has previously had success in verifying natural product structures through the application of ^{1}H and ^{13}C DFT-NMR calculations.[17-19] To calculate theoretical NMR shielding constants for both possible isomers (*ortho* and *para*) of **7**, their structures were subject to molecular mechanics energy minimization and conformational searches using MMFFs.[20] Both isomers yielded a number of minimum energy conformers, which were each minimized using DFT with the B3LYP/6-31+G(d,p) functional and basis set combination.[21-24] The shielding constants were then obtained through single-point calculations using the MPW1PW91/6-311+G(2d,p) as described in the experimental section.[25,26] A linear regression model was used to scale the calculated shielding constants, providing ^{1}H and ^{13}C NMR shifts for both the *ortho* and *para* forms of 7 (Table 3). The reported values are the Boltzmann-weighted averages of all values obtained for the conformers identified for the *ortho* and *para* cases (see Experimental).

Analysis of the theoretical ^{1}H and ^{13}C NMR data showed that the *para* form of **7** was the correct isomer. The mean absolute deviation (MAD) values for both the *ortho* and *para* forms were below 5 ppm in the ^{13}C NMR data, which is considered within the range of an acceptable DFT-NMR calculation for theoretical values.[17-19,27] However, the MAD of the *para* form was significantly lower (2.1 ppm), less than half that of the *ortho* form (4.4 ppm), indicating that the theoretical ^{13}C NMR *para* data was in better agreement with the experimental ^{13}C NMR data. The theoretical ^{1}H and ^{13}C NMR data was also analyzed

through the DP4 statistical analysis, which can be used to distinguish between constitutional isomers.[28,29] The DP4 analysis showed that, when considered together, the ^{1}H and ^{13}C NMR data was most consistent with the *para* isomer (100% probability). Thus, the structure of **7**, as well as the proton-poor anthraquinone core of the other metabolites, was unambiguously determined.

CONCLUSIONS

A chemical investigation of a specimen of the Australian marine sponge, *Clathria hirsuta*, has led to the isolation and characterization of six polyketide-derived anthraquinones (**1**–**6**). In addition to describing four new anthraquinones (**3**–**6**), we were able to complete the spectroscopic characterization of the known compounds rhodocomatulin 5,7-dimethyl ether (**1**) and rhodocomatulin 7-methyl ether (**2**). A secondary investigation of the crinoid, *Comatula rotalaria*, yielded further amounts of **1** and **2**, and two additional and new compounds, **7** and **8**. We were particularly intrigued to discover the presence of the rhodocomatulin class of anthraquinones in a marine sponge, as they had only previously been reported from marine featherstars. This may raise questions about the biosynthetic origin of the metabolites in the sponge, possibly indicating that they are products of a microbial symbiont or are originally crinoid metabolites that are accumulated within sponge tissues over time.[30]

EXPERIMENTAL SECTION

General Experimental Procedures. All UV spectra were recorded on a JASCO V-650 UV/Vis spectrophotometer. IR Spectra were recorded on a Bruker Tensor 27 spectrophotometer (Billerica, MA, USA). All NMR spectra were recorded on either Varian or Bruker NMR instruments. Varian: spectra recorded at 30°C on a 500 MHz Unity INOVA spectrometer. Bruker: spectra recorded at 25°C on an 800 or 900 MHz NMR, which were both equipped with triple resonance cold probes. The ^{1}H and ^{13}C NMR chemical shifts were

referenced to the solvent peaks for DMSO-d_6 at δ_H 2.50 and δ_C 39.5. LRESIMS data were recorded on a Waters LC-MS system equipped with a Phenomenex Luna C_{18} column (3 μm, 100 Å, 4.6 × 50 mm), a PDA detector, and a ZQ ESI mass spectrometer. The HRESIMS data were recorded on a Bruker MicroToF-Q spectrometer (Dionex UltiMate 3000 micro LC system, ESI mode). Alltech Davisil DIOL-bonded silica (30–40 μm, 60 Å) or Alltech Davisil C_{18}-bonded silica (35–75 μm, 150 Å) was used for preadsorption and flash column purifications. The preadsorbed extracts/fractions were packed into Alltech stainless steel guard cartridges (10 × 30 mm, Columbia, MD, USA). A Waters 600 pump equipped with a Waters 966 PDA detector and Gilson 715 liquid handler were used for all semipreparative HPLC work. For NP-HPLC work, a YMC DIOL (5 μm, 120 Å, 150 × 20 mm) column was used. For RP-HPLC, a Phenomenex Luna 5 μm 100 Å C_{18} column (10 mm × 250 mm) was used. All solvents used for chromatography, UV, and MS were Lab-Scan HPLC grade, and the H_2O was Millipore Milli-Q PF filtered. A Bioline orbital shaker was used for all large-scale extractions of sponge material.

Animal Material. The specimen of *Clathria (Thalysias) hirsuta* Hooper and Lévi, 1993 was collected at a depth of 31 m by trawl on the Department of Primary Industries & Fisheries (DPI) Research Vessel "Gwendoline May" between Boulder and Vicki Harriott Reef, off Cooktown, Queensland, Australia during October of 2004. A voucher specimen (G330140) was deposited at the Queensland Museum, South Brisbane, Queensland, Australia. All samples were collected under the Great Barrier Reef Marine Parks Permit G03/10637.1 and DPI General Fisheries Permit PRM02988B. The sample was immediately frozen upon collection and stored in a –20°C freezer, before being freighted to the Eskitis Institute where it was freeze-dried and ground into a fine powder. The featherstar specimen, *Comatula (Validia) rotalaria* Lamarck, 1816 (one large collection divided into two samples, TS8000776 and TS8000777) was collected via trawl by the DPI RV "Gwendoline May" in

the Torres Strait (an Australian territory situated between Northern Queensland and Papua New Guinea) at a depth of 15 m in January 2004, with the same collection permit details described above. The crinoids were immediately immersed in a 70:30 EtOH/H_2O solution, and stored in a dark, temperature controlled environment (~25°C). Voucher specimens TS80000776 and TS80000777 have been deposited at the Queensland Museum, Brisbane, Australia.

Extraction and Isolation. The freeze-dried and ground *C. hirsuta* specimen (21 g) was extracted exhaustively with CH_2Cl_2 (2 × 500 mL) and MeOH (2 × 500 mL). The yellow/white CH_2Cl_2 extract was found to contain predominantly fatty acids/lipids by ^1H NMR, and was therefore discarded. The MeOH extract was dried to give a reddish gum (5.2 g), which was then pre-adsorbed onto DIOL-bonded silica. The extract was then purified by a DIOL-bonded silica flash column (60 × 40 mm), eluting with a 20% stepwise gradient from *n*-hexane to EtOAc, followed by 100% MeOH (100 mL of solvent/step), which yielded 7 fractions. The 60:40, 80:20 and 100:0 EtOAc/*n*-hexane fractions (i.e., fractions 4–6) were combined (~ 53.0 mg) and preadsorbed onto ~1 g DIOL-bonded silica, then added to a guard cartridge that was subsequently attached to a semi-preparative DIOL HPLC column. Isocratic conditions of *n*-hexane were held for the first 10 min, followed by a linear gradient to 20% *i*-PrOH/80% *n*-hexane for 40 min, then held for a further 10 min at 20% *i*-PrOH/80% *n*-hexane, all at a flowrate of 9 mL/min. 120 fractions (0.5 min each) were collected from the start of the HPLC run. Fractions 75, 80, and 105 contained pure rhodocomatulin 7-methyl ether (**2**, 0.3 mg, 0.0014% dry wt), 6-methoxy-rhodocomatulin 7-dimethyl ether (**3**, 0.1 mg, 0.0005% dry wt), and rhodocomatulin 5,7-dimethyl ether (**1**, 1.6 mg, 0.0076% dry wt), respectively. The 100% MeOH fraction (0.6 g) from the DIOL flash column was preadsorbed onto C_{18}-bonded silica. This was subjected to RP-HPLC using a linear gradient from 10:90 MeOH/H_2O/0.1% TFA to 100% MeOH/0.1% TFA over 160 min, then held at 100%

MeOH/0.1% TFA for a further 30 minutes, all at a flow rate of 9 mL/min. 190 timed fractions (190 × 1 min) were collected from the start of the HPLC run. Fractions 123, 135 and 141 were found to contain 3-bromo-6-methoxy-12-desethyl-rhodocomatulin 7-methyl ether (**4**, 0.6 mg, 0.0029% dry wt), 3-bromo-6-methoxy-rhodocomatulin 7-methyl ether (**5**, 0.5 mg, 0.0023% dry wt) and 3-bromo-rhodocomatulin 7-methyl ether (**6**, 0.4 mg, 0.0019% dry wt), respectively.

The EtOH/H_2O (70:30) extracts of *Comatula* rotalaria (TS80000776 and TS80000777) were combined (600 mL) because they were subdivisions of the same collection, and also had essentially identical LC-MS traces. Thus, 600 mL of an EtOH/H_2O (70:30) extract of *C. rotalaria* (~100 g, wet wt) was dried by rotary evaporation to yield 1.41 g of a red gum. This was then pre-adsorbed onto DIOL-bonded silica (~1 g). The extract was then purified by DIOL-bonded silica flash column chromatography (60 × 40 mm), utilizing a 20% stepwise gradient from *n*-hexane to EtOAc, followed by 100% MeOH (100 mL of solvent/step), which yielded 7 fractions. The 40:60, 60:40 and 80:20 EtOAc/*n*-hexane fractions (i.e., fractions 3–5) were combined (~ 76 mg) and subjected to NP-HPLC. These combined fractions were pre-adsorbed onto ~1 g DIOL-bonded silica, and then added to a guard cartridge that was attached to a DIOL semi-preparative HPLC column. Isocratic conditions of *n*-hexane were held for the first 10 min, followed by a linear gradient to 20% *i*-PrOH/80% *n*-hexane for 40 min, then held for a further 10 min at 20% *i*-PrOH/80% *n*-hexane, all at a flow rate of 9 mL/min. 120 timed fractions (120 × 0.5 min) were collected from the start of the HPLC run. UV-active fractions were analyzed by LC-MS and ^{1}H NMR spectroscopy. Fractions 70–75 and fractions 109–111 were found to contain further amounts of rhodocomatulin 7-methyl ether (**2**, 5.0 mg, 0.005% dry wt) and rhodocomatulin 5,7-dimethyl ether (**1**, 8.0 mg, 0.008% dry wt). Fractions 108-111 and 80-81 contained the new compounds 12-desethyl-

rhodocomatulin 5,7-dimethyl ether (**7**, 0.9 mg, 0.0009% dry wt) and 12-desethyl-rhodocomatulin 7-methyl ether (**8**, 1.0 mg, 0.001% dry wt) respectively.

*Rhodocomatulin 5,7-dimethyl ether (**1**):* Bright orange gum; UV (MeOH) λ_{max} (log ε) 220 (3.46), 264 (3.20), 313 (3.27), 468 (2.62) nm; IR (ν_{max}) 3533, 1667, 1621, 1589, 1552, 1386, 1328, 1249, 1136, 1031, 948, 760, 504 cm^{-1}; ^{1}H and ^{13}C NMR data (DMSO-d_6 + trace TFA, 900 MHz), see Table 1 and 2; (–)-LRESIMS *m/z* 369 $[M - H]^-$; (–)-HRESIMS *m/z* 369.0984 $[M - H]^-$ (calcd. for $C_{20}H_{17}O_7$, 369.0980).

*Rhodocomatulin 7-methyl ether (**2**):* Pink powder; UV (MeOH) λ_{max} (log ε) 264 (3.84), 318 (3.94), 517 (3.31) nm; IR (ν_{max}) 3500 (br), 1703, 1625, 1601, 1438, 1380, 1250, 1187, 1165, 1147, 1024, 1001, 735, 657 cm^{-1}; ^{1}H and ^{13}C NMR data (DMSO-d_6 + trace TFA, 500 MHz), see Table 1 and 2; (–)-LRESIMS *m/z* 355 $[M - H]^-$; (–)-HRESIMS *m/z* 355.0822 $[M - H]^-$ (calcd. for $C_{19}H_{15}O_7$, 355.0823).

*6-Methoxy-rhodocomatulin 7-dimethyl ether (**3**):* Orange gum; UV (MeOH) λ_{max} (log ε) 260 (3.39), 318 (3.44), 500 (2.89) nm; ^{1}H and ^{13}C NMR data (DMSO-d_6 + trace TFA, 900 MHz), see Table 1 and 2; (–)-LRESIMS *m/z* 385 $[M - H]^-$; (–)-HRESIMS *m/z* 385.0926 $[M - H]^-$ (calcd. for $C_{20}H_{17}O_8$, 385.0929).

*3-Bromo-6-methoxy-12-desethyl-rhodocomatulin 7-methyl ether (**4**):* Brown/red gum; UV (MeOH) λ_{max} (log ε) 324 (3.12), 515 (2.44), 517 (3.31) nm; ^{1}H and ^{13}C NMR data (DMSO-d_6 + trace TFA, 900 MHz), see Table 1 and 2; (–)-LRESIMS *m/z* 435 $[M - H]^-$ 100%, 437 $[M - H]^-$ 100%; (–)-HRESIMS *m/z* 434.9714 $[M - H]^-$ (calcd. for $C_{19}H_{15}{}^{79}BrO_7$, 434.9721).

*3-Bromo-6-methoxy-rhodocomatulin 7-methyl ether (**5**):* Orange gum; UV (MeOH) λ_{max} (log ε) 219 (3.81), 261 (3.59), 322 (3.80), 425 (3.06), 521 (3.09) nm; ^{1}H and ^{13}C NMR data (DMSO-d_6 + trace TFA, 900 MHz), see Table 1 and 2; (–)-LRESIMS *m/z* 463 $[M - H]^-$ 100%, 465 $[M - H]^-$ 100%; (–)-HRESIMS *m/z* 463.0029 $[M - H]^-$ (calcd. for $C_{20}H_{16}{}^{79}BrO_8$, 463.0034).

*3-Bromo-rhodocomatulin 7-methyl ether (**6**):* Red gum; UV (MeOH) λ_{max} (log ε) 265 (3.34), 318 (3.50), 520 (2.83) nm; ^{1}H and ^{13}C NMR data (DMSO-d_6 + trace TFA, 900 MHz), see Table 1 and 2; (–)-LRESIMS *m/z* 433 $[M - H]^-$ 100%, 435 $[M - H]^-$ 100%, (–)-HRESIMS *m/z* 432.9928 $[M - H]^-$ (calcd. for $C_{19}H_{14}{}^{79}BrO_7$, 432.9928).

*12-Desethyl-rhodocomatulin 5,7-dimethyl ether (**7**):* orange/yellow gum; UV (MeOH) (log ε) 260 (3.09), 315 (3.11), 514 (2.51) nm; ^{1}H and ^{13}C NMR data (DMSO-d_6 + trace TFA, 800 MHz), see Table 3; (–)-LRESIMS *m/z* 341 $[M - H]^-$, (–)-HRESIMS *m/z* 341.0668 $[M - H]^-$ (calcd. for $C_{18}H_{14}O_7$, 341.0667).

*12-Desethyl-rhodocomatulin 7-methyl ether (**8**):* orange gum; UV (MeOH) (log ε) 257 (3.06), 309 (2.91) nm; ^{1}H and ^{13}C NMR data (DMSO-d_6 + trace TFA, 800 MHz), see Table 3; (–)-LRESIMS *m/z* 327 $[M - H]^-$, (–)-HRESIMS *m/z* 327.0512 $[M - H]^-$ (calcd. for $C_{17}H_{11}O_7$, 327.0510)

Computational Chemistry

Monte Carlo Conformational searching was performed using Macromodel v10.4 for compounds of interest. Torsional sampling (MCMM) was performed with 1000 steps per rotatable bond. Each step was minimised with the MMFFs force field using TNCG method with maximum iterations of 50,000 and energy convergence threshold of 0.02. Mirror image conformations were not retained and all other parameters were left as the default values. The low energy conformations (< 3 kcal/mol from global minimum) were further optimised using DFT calculations in Gaussian. All calculations were performed using Gaussian 09W[31] software package on a windows workstation (Windows Server 2008, service pack 1, 64-bit). All compounds were initially optimized in gas phase using the B3LYP/6-31+G(d,p)[24,32-34] level of theory. This combination has been previously shown to provide accurate geometries for organic molecules at a reasonable low computational cost.[35] For all optimizations the vibrational frequencies were checked for imaginary frequencies to assure all final geometries

corresponded to a true minimum on the electronic potential energy surface. The NMR isotropic shielding tensors were calculated from a single point calculation using the pre-optimized structures, method above, with the MPW1PW91/6-311+G(2d,p) functional and basis set reported in the literature. The functional and basis set was selected for the solvent from the recently published work of Pierens [36]. The isotropic magnetic shielding tensors were computed using the gauge-independent atomic orbital (GIAO)[37] methodology and the isotropic magnetic shielding tensors were averaged over all symmetry related carbons and hydrogens where applicable. The isotropic magnetic shielding tensors were calculated with the inclusion of solvent. The effect of solvent was investigated via the inclusion of the polarizable continuum model (IEF-PCM).[38] All conformers were further optimised using a larger basis set (B3LYP/6-31+G(d,p)) to obtain the energies which were used in the calculation of average chemical shift using a Boltzmann distribution. The output files were process using a PowerShell scripts on the windows workstation and the scaling factors previously reported were used to convert the NMR isotropic shielding tensor to a chemical shift and to extract the coupling constant data.

Cell Proliferation Studies

H460, MCF-7 and SF268 cells were grown in 10% RPMI 1640 supplemented with foetal bovine serum (10%). Cells were then seeded into 96-well culture plates (100 μL) and incubated overnight (37 °C) in a humidified 5% CO_2, 95% air atmosphere. For the single dose study, rhodocomatulin 5,7-dimethyl ether (**1**) was dissolved to a concentration of 10 mM in DMSO, then diluted in medium to 20 μM. 100 μL of **1** was then added to each of 3 wells of each plate (final concentration = 10 μM). The plates were then incubated for a further 72 h, after which viable cells were measured using the sulforhodamine B assay.[39,40] Briefly, the cells were fixed in 2% cold trichloroacetic acid (1 h, 4°C) and plates were then rinsed with distilled H_2O. Following this, they were left to air dry and then stained with 0.4%

SRB (Aldrich) in 1% acetic acid (v/v) for 30 min. The unbound dye was removed by washing twice with distilled H_2O and then 1% acetic acid. Protein-bound dye was solubilized in unbuffered Tris base (10 mM) and the absorbance read at 550 nm using a Versamax automatic plate reader. The percentage cell proliferation was then calculated for each plate as the mean absorbance of the drug treated wells relative to that of the relevant control cells × 100.

ASSOCIATED CONTENT

Supporting Information.

1D and 2D NMR spectra for compounds **1**–**8**, HPLC chromatograms, proposed biosynthetic scheme and further DFT-NMR details are provided in the supporting information. The Supporting Information is available free of charge on the ACS Publications website at DOI:

AUTHOR INFORMATION

Corresponding Author

* Tel: +61-7-3735-6043. E-mail: r.davis@griffith.edu.au * Tel: +61-7-3735-8367. E-mail: y.feng@griffith.edu.au

Notes

The authors declare no competing financial interest.

ACKNOWLEDGEMENTS

We thank G. MacFarlane from the University of Queensland for acquiring HRESIMS measurements. We would also like to thank the Centre for Advanced Imaging (University of Queensland) for access to the 900 MHz NMR spectrometer. A special thanks to Dr Carleen Cullinane from the Peter MacCallum Centre, Melbourne for conducting the cell proliferation studies. S.K. would like to acknowledge the Australian Government for an Australian Postgraduate Award (APA) scholarship. R.A.D. and Y.F. would like to acknowledge the National Health and Medical Research Council (NHMRC, Grant APP1024314) and the

Australian Research Council (ARC) for support toward NMR and MS equipment (Grants LE0668477 and LE0237908).

REFERENCES

(1) Blunt, J. W.; Copp, B. R.; Keyzers, R. A.; Munro, M. H. G.; Prinsep, M. R. *Nat. Prod. Rep.* **2015**, *32*, 116-211.

(2) Woo, J.-K.; Kim, C.-K.; Kim, S.-H.; Kim, H.; Oh, D.-C.; Oh, K.-B.; Shin, J. *Org. Lett.* **2014**, *16*, 2826-2829.

(3) Woo, J.-K.; Kim, C.-K.; Ahn, C.-H.; Oh, D.-C.; Oh, K.-B.; Shin, J. *J. Nat. Prod.* **2015**, *78*, 218-224.

(4) Capon, R. J.; Miller, M.; Rooney, F. *J. Nat. Prod.* **2001**, *64*, 643-644.

(5) El-Naggar, M.; Conte, M.; Capon, R. J. *Org. Biomol. Chem.* **2010**, *8*, 407-412.

(6) Wei, X.; Henriksen, N. M.; Skalicky, J. J.; Harper, M. K.; Cheatham, T. E.; Ireland, C. M.; Van Wagoner, R. M. *J. Org. Chem.* **2011**, *76*, 5515-5523.

(7) Davis, R. A.; Mangalindan, G. C.; Bojo, Z. P.; Antemano, R. R.; Rodriguez, N. O.; Concepcion, G. P.; Samson, S. C.; de Guzman, D.; Cruz, L. J.; Tasdemir, D.; Harper, M. K.; Feng, X.; Carter, G. T.; Ireland, C. M. *J. Org. Chem.* **2004**, *69*, 4170-4176.

(8) Capon, R. J.; Miller, M.; Rooney, F. *J. Nat. Prod.* **2000**, *63*, 821-824.

(9) Simoneau, B.; Brassard, P. *J. Nat. Prod.* **1987**, *50*, 1080-1082.

(10) Sutherland, M.; Wells, J. *Aust. J. Chem.* **1967**, *20*, 515-533.

(11) Cao, S.; Clardy, J. *Tetrahedron Lett.* **2011**, *52*, 2206-2208.

(12) Ishikawa, Y.; Ishibashi, M.; Yamamoto, Y.; Hayashi, M.; Komiyama, K. *Chem. Pharm. Bull.* **2002**, *50*, 1126-1127.

(13) Shintani, A.; Yamazaki, H.; Yamamoto, Y.; Ahmed, F.; Ishibashi, M. *Chem. Pharm. Bull.* **2009**, *57*, 894-895.

(14) Davis, R. A.; Baron, P. S.; Neve, J. E.; Cullinane, C. *Tetrahedron Lett.* **2009**, *50*, 880-882.

(15) Yin, S.; Cullinane, C.; Carroll, A. R.; Quinn, R. J.; Davis, R. A. *Tetrahedron Lett.* **2010**, *51*, 3403-3405.

(16) Aiello, A.; Fattorusso, E.; Luciano, P.; Mangoni, A.; Menna, M. *Eur. J. Org. Chem.* **2005**, *2005*, 5024-5030.

(17) Khokhar, S.; Feng, Y.; Campitelli, M. R.; Ekins, M. G.; Hooper, J. N.; Beattie, K. D.; Sadowski, M. C.; Nelson, C. C.; Davis, R. A. *Bioorg. Med. Chem. Lett.* **2014**, *24*, 3329-3332.

(18) Khokhar, S.; Feng, Y.; Campitelli, M. R.; Quinn, R. J.; Hooper, J. N.; Ekins, M. G.; Davis, R. A. *J. Nat. Prod.* **2013**, *76*, 2100-2105.

(19) Khokhar, S.; Feng, Y.; Carroll, A. R.; Campitelli, M. R.; Quinn, R. J.; Hooper, J. N.; Ekins, M. G.; Davis, R. A. *Tetrahedron* **2015**, *71*, 6204-6209.

(20) Halgren, T. A. *J. Comput. Chem.* **1999**, *20*, 720-729.

(21) Becke, A. D. *J. Chem. Phys.* **1993**, *98*, 5648-5652.

(22) Lee, C.; Yang, W.; Parr, R. G. *Phys. Rev. B.* **1988**, *37*, 785-789.

(23) Vosko, S. H.; Wilk, L.; Nusair, M. *Can. J. Phys.* **1980**, *58*, 1200-1211.

(24) Stephens, P.; Devlin, F.; Chabalowski, C.; Frisch, M. J. *The Journal of Physical Chemistry* **1994**, *98*, 11623-11627.

(25) Marten, B.; Kim, K.; Cortis, C.; Friesner, R. A.; Murphy, R. B.; Ringnalda, M. N.; Sitkoff, D.; Honig, B. *J. Phys. Chem.* **1996**, *100*, 11775-11788.

(26) Tannor, D. J.; Marten, B.; Murphy, R.; Friesner, R. A.; Sitkoff, D.; Nicholls, A.; Honig, B.; Ringnalda, M.; Goddard, W. A. *J. Am. Chem. Soc.* **1994**, *116*, 11875-11882.

(27) Palazzo, T. A.; Truong, T. T.; Wong, S. M. T.; Mack, E. T.; Lodewyk, M. W.; Harrison, J. G.; Gamage, R. A.; Siegel, J. B.; Kurth, M. J.; Tantillo, D. J. *J. Chem. Ed.* **2015**, *92*, 561-566.

(28) Menna, M.; Aiello, A.; D'Aniello, F.; Imperatore, C.; Luciano, P.; Vitalone, R.; Irace, C.; Santamaria, R. *Eur. J. Org. Chem.* **2013**, *2013*, 3241-3246.

(29) Smith, S. G.; Goodman, J. M. *J. Am. Chem. Soc.* **2010**, *132*, 12946-12959.

(30) Perez, T.; Wafo, E.; Fourt, M.; Vacelet, J. *Environ. Sci. Technol.* **2003**, *37*, 2152-2158.

(31) Gaussian 09, R. D., M. J. Frisch, G. W. Trucks, H. B. Schlegel, G. E. Scuseria, M. A. Robb, J. R. Cheeseman, G. Scalmani, V. Barone, B. Mennucci, G. A. Petersson, H. Nakatsuji, M. Caricato, X. Li, H. P. Hratchian, A. F. Izmaylov, J. Bloino, G. Zheng, J. L. Sonnenberg, M. Hada, M. Ehara, K. Toyota, R. Fukuda, J. Hasegawa, M. Ishida, T. Nakajima, Y. Honda, O. Kitao, H. Nakai, T. Vreven, J. A. Montgomery, Jr., J. E. Peralta, F. Ogliaro, M. Bearpark, J. J. Heyd, E. Brothers, K. N. Kudin, V. N. Staroverov, T. Keith, R. Kobayashi, J. Normand, K. Raghavachari, A. Rendell, J. C. Burant, S. S. Iyengar, J. Tomasi, M. Cossi, N. Rega, J. M. Millam, M. Klene, J. E. Knox, J. B. Cross, V. Bakken, C. Adamo, J. Jaramillo, R. Gomperts, R. E. Stratmann, O. Yazyev, A. J. Austin, R. Cammi, C. Pomelli, J. W. Ochterski, R. L. Martin, K. Morokuma, V. G. Zakrzewski, G. A. Voth, P. Salvador, J. J. Dannenberg, S. Dapprich, A. D. Daniels, O. Farkas, J. B. Foresman, J. V. Ortiz, J. Cioslowski, and D. J. Fox, Gaussian, Inc., Wallingford CT, 2013., Ed.

(32) Becke, A. D. *J. Chem. Phys.* **1993**, *98*, 1372-1377.

(33) Lee, C.; Yang, W.; Parr, R. G. *Phys. Rev. B.* **1988**, *37*, 785.

(34) Tirado-Rives, J.; Jorgensen, W. L. *J. Chem. Theory Comput.* **2008**, *4*, 297-306.

(35) Lodewyk, M. W.; Siebert, M. R.; Tantillo, D. J. *Chem. Rev.* **2011**, 1839-1862.

(36) Pierens, G. K. *J. Comput. Chem.* **2014**, *35*, 1388-1394.

(37) Cheeseman, J. R.; Trucks, G. W.; Keith, T. A.; Frisch, M. J. *J. Chem. Phys.* **1996**, *104*, 5497-5509.

(38) Bandyopadhyay, P.; Gordon, M. S.; Mennucci, B.; Tomasi, J. *J. Chem. Phys.* **2002**, *116*, 5023-5032.

(39) Monks, A.; Scudiero, D.; Skehan, P.; Shoemaker, R.; Paull, K.; Vistica, D.; Hose, C.; Langley, J.; Cronise, P.; Vaigro-Wolff, A. *J. Natl. Cancer Inst.* **1991**, *83*, 757-766.

(40) Skehan, P.; Storeng, R.; Scudiero, D.; Monks, A.; McMahon, J.; Vistica, D.; Warren, J. T.; Bokesch, H.; Kenney, S.; Boyd, M. R. *J. Natl. Cancer Inst.* **1990**, *82*, 1107-1112.

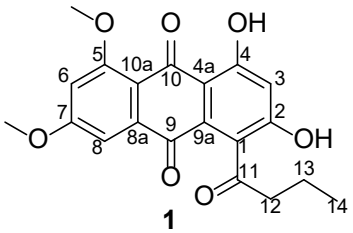
O
O
OH
5
10a
4a
4
6
10
3
7
9
2
8
8a
9a
1
OH
O
11
13
O
12
14

1

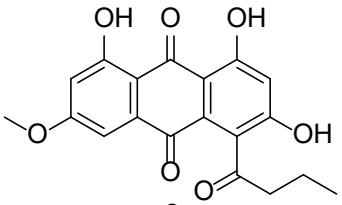
OH
O
OH
O
OH
O
O

2

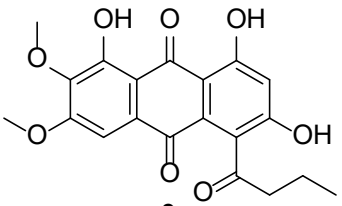
OH
O
OH
O
O
OH
O
O

3

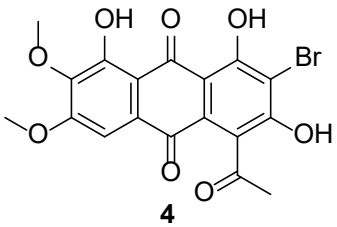
OH
O
OH
O
Br
O
OH
O
O

4

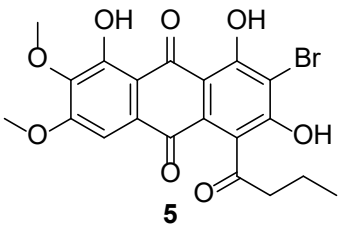
OH
O
OH
O
Br
O
OH
O
O

5

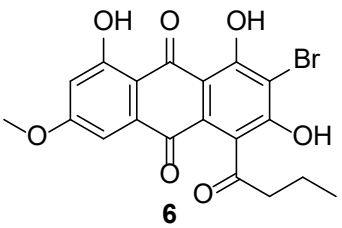
OH
O
OH
O
Br
O
OH
O
O

6

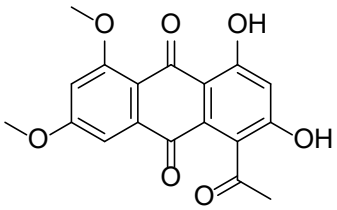
O
O
OH
O
OH
O
O

7

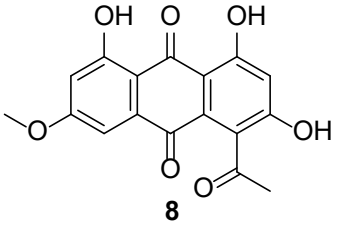
OH
O
OH
O
OH
O
O

8

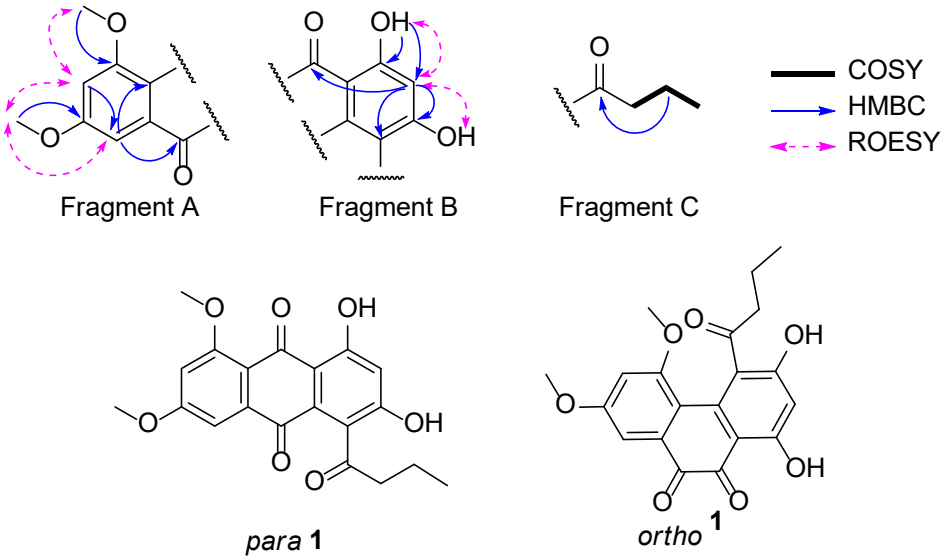

Figure 1. The fragments of **1** established through NMR analysis, and the two candidate structures that were identified: *ortho* and *para* forms.

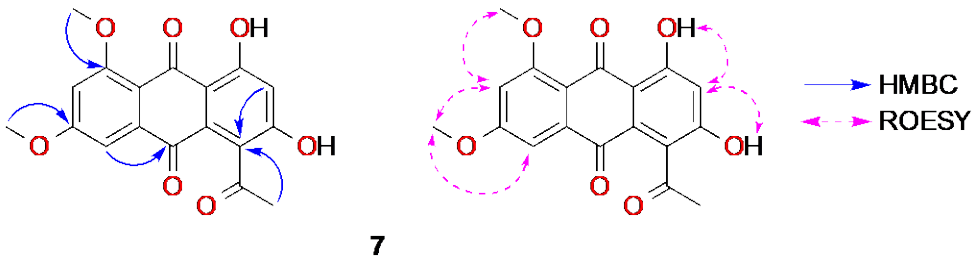

Figure 2. Key 2D NMR correlations for compound **7**

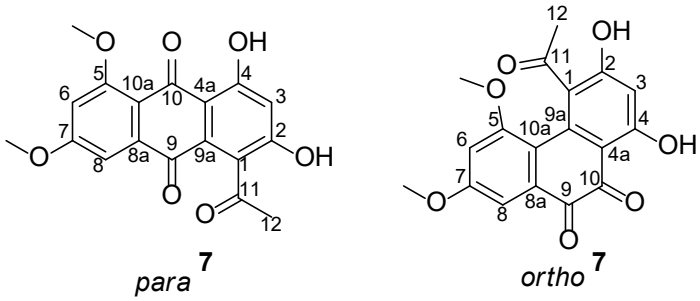

Figure 3. The two possible forms of compound **7**

Table 1. ^{1}H NMR Data for Anthraquinones **1**–**6**

	δ_H, mult. (*J* in Hz)[a]					
Position	**1**[b]	**2**[c]	**3**[b]	**4**[b]	**5**[b]	**6**[b]
2-OH	11.33, br s	11.64, br s	11.70, br s	11.93, br s	11.94, br s	12.01, br s
3	6.66, s	6.69, s	6.69, s	-	-	-
4-OH	13.61, s	12.38, s	12.29, s	12.29, s	13.19, s	13.31, s
5-OH	-	12.15, s	12.10, s	[d]	[d]	[d]
5-OMe	3.96, s	-	-	-	-	-
6	7.04, d (2.5)	6.86, d (2.6)	-	-	-	6.91, d (2.5)
6-OMe	-	-	3.85, s	3.85, s	3.85, s	-
7-OMe	3.97, s	3.92, s	3.99, s	3.99, s	3.99, s	3.93, s
8	7.22, d (2.5)	7.12, d (2.6)	7.33, s	7.37, s	7.34, s	7.16, d (2.5)
12	2.64, br t (7.6)	2.62, br t (7.6)	2.62, br t (7.6)	2.42, s	2.65, br t (7.6)	2.64, br t (7.6)
13	1.67, qt (7.6, 7.6)	1.69, qt (7.6, 7.6)	1.70, qt (7.6, 7.6)	-	1.71, qt (7.6, 7.6)	1.71, qt (7.6, 7.6)
14	0.98, t (7.6)	0.97, t (7.6)	0.97, t (7.6)	-	0.97, t (7.6)	0.98, t (7.6)

[a] Spectra acquired in DMSO-d_6 + trace TFA
[b] 900 MHz
[c] 500 MHz
[d] Not observed

Table 2. ^{13}C NMR Data for Anthraquinones **1**–**6**

	δ_C, type[a]					
Position	**1**[b]	**2**[c]	**3**[b,d]	**4**[b,d]	**5**[b,d]	**6**[b,d]
1	124.9, C	126.6, C	126.8, C	[e]	[e]	[e]
2	159.9, C	161.5, C	[e]	[e]	[e]	[e]
3	108.6, CH	108.0, CH	107.8, CH	106.1, C[h]	105.9, C[i]	105.9, C[j]
4	163.8, C	163.7, C	163.7, C	160.3, C	160.7, C	160.7, C
4a	109.8, C	108.2, C	108.4, C	108.8, C[h]	108.8, C[i]	108.8, C[j]
5	162.8, C	163.9, C	155.3, C	[e]	[e]	[e]
5-OMe	56.2, CH_3	-	-	-	-	-
6	105.1, CH	106.9, CH	141.2, C	141.5, C	141.4, C	107.3, CH
6-OMe	-	-	60.1, CH_3	60.6, CH_3	60.1, CH_3	-
7	164.8, C	165.8, C	158.0, C	158.3, C	158.2, C	166.0, C
7-OMe	56.7, CH_3	56.1, CH_3	56.3, CH_3	56.7, CH_3	56.8, CH_3	56.7, CH_3
8	104.7, CH	107.4, CH	104.4, CH	105.0, CH	104.9, CH	108.0, CH
8a	130.2, C[f]	131.0, C[g]	[e]	[e]	128.4, C	[e]
9	182.5, C	181.6, C	180.9, C	181.1, C	181.0, C	[e]
9a	136.2, C[f]	134.3, C[g]	[e]	[e]	[e]	[e]
10	185.2, C	188.8, C	[e]	[e]	[e]	[e]
10a	113.6, C	109.4, C	111.0, C	111.3, C	111.2, C	108.6, C
11	203.4, C	203.1, C	[e]	200.4, C	[e]	[e]
12	44.7, CH_2	44.4, CH_2	44.2, CH_2	31.0, CH_3	44.5, CH_2	44.5, CH_2
13	16.2, CH_2	16.4, CH_2	16.2, CH_2	-	16.6, CH_2	16.7, CH_2
14	13.6, CH_3	13.5, CH_3	13.3, CH_3	-	13.7, CH_3	13.7, CH_3

[a] Spectra acquired in DMSO-d_6 + trace TFA
[b] 225 MHz
[c] 125 MHz
[d] ^{13}C NMR shift obtained from HSQC and HMBC spectra
[e] Not observed
[f-g] Signals are interchangeable

Table 3. ^{1}H and ^{13}C NMR Data for Anthraquinones **7** and **8**[a]

Position	**7**[b]	**7**[c]	**8**[b]	**8**[c]
	δ_H, mult. (*J* in Hz)	δ_C, type	δ_H, mult. (*J* in Hz)	δ_C, type
1		124.9, C		126.6, C
2		159.7, C		161.2, C
2-OH	11.37, br s	-	11.68, br s	-
3	6.67, s	108.5, CH	6.70, s	108.1, CH
4		163.8, C		163.5, C
4-OH	13.58, s	-	12.37, s	-
4a		109.3, C		108.1, C
5		162.8, C		163.8, C
5-OH		-	12.18, s	-
5-OMe	3.96, s	56.1, CH_3		
6	7.04, d (2.5)	104.9, CH	6.89, d (2.5)	107.0, CH
7		164.8, C		165.7, C
7-OMe	3.97, s	56.6, CH_3	3.92, s	56.1, CH_3
8	7.24, d (2.5)	104.6, CH	7.16, d (2.5)	107.4, CH
8a		130.0, C[d]		130.9, C[e]
9		182.5, C		181.8, C
9a		136.1, C[d]		134.3, C[e]
10		185.7, C		188.9, C
10a		113.4, C		109.5, C
11		201.2, C		201.2, C
12	2.39, s	30.5, CH_3	2.40, s	30.8, CH_3

[a] Spectra acquired in DMSO-d_6 + trace TFA
[b] 800 MHz
[c] 200 MHz
[d–e] Signals are interchangeable

Table 4. DFT NMR Shifts for *ortho* and *para* Anthraquinone (**7**)[a]

Position	**7** $^{1}H_{exp}$	**7 (*ortho*)** $^{1}H_{theo}$	**7 (*para*)** $^{1}H_{theo}$	**7** $^{13}C_{exp}$	**7 (*ortho*)** $^{13}C_{theo}$	**7 (*para*)** $^{13}C_{theo}$
1				124.9	113.5	116.5
2				159.7	167.1	161.6
3	6.67	6.11	6.52	108.5	100.4	109.0
4				163.8	167.7	165.3
4a				109.3	109.7	110.0
5				162.8	157.2	161.4
5-OMe	3.96	3.76	3.84	56.1	53.8	53.0
6	7.04	6.67	6.70	104.9	106.7	104.9
7				164.8	161.1	163.6
7-OMe	3.97	3.50	3.79	56.6	53.2	53.4
8	7.24	7.25	7.32	104.6	109.7	104.9
8a				130.0[b]	131.7	134.1
9				182.5	181.0	183.6
9a				136.1[b]	142.2	135.1
10				185.7	177.5	183.7
10a				113.4	117.7	112.3
11				201.2	203.2	206.4
12	2.39	2.12	2.37	30.5	28.3	31.5
MD		0.56	0.34		11.4	8.4
MAD		0.31	0.15		4.4	2.1

	***ortho* (7)**	***para* (7)**
DP4 (^{1}H only)	9.3%	90.7%
DP4 (^{13}C only)	0.0%	100.0%
DP4 (^{1}H and ^{13}C)	0.0%	100.0%

[a] Exchangeable signals not included in calculations

[b] These chemical shifts are interchangeable. They have been matched with the experimental ^{13}C atom which best minimizes the MAD.